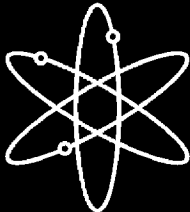


**A Combined Analytical Study to  
Characterize Uranium Soil and  
Sediment Contamination:  
The Case of the Naturita  
UMTRA Site and the  
Role of Grain Coatings**



**Sandia National Laboratories**



**U.S. Nuclear Regulatory Commission  
Office of Nuclear Regulatory Research  
Washington, DC 20555-0001**



**AVAILABILITY OF REFERENCE MATERIALS  
IN NRC PUBLICATIONS**

**NRC Reference Material**

As of November 1999, you may electronically access NUREG-series publications and other NRC records at NRC's Public Electronic Reading Room at <http://www.nrc.gov/reading-rm.html>. Publicly released records include, to name a few, NUREG-series publications; *Federal Register* notices; applicant, licensee, and vendor documents and correspondence; NRC correspondence and internal memoranda; bulletins and information notices; inspection and investigative reports; licensee event reports; and Commission papers and their attachments.

NRC publications in the NUREG series, NRC regulations, and *Title 10, Energy*, in the Code of *Federal Regulations* may also be purchased from one of these two sources.

1. The Superintendent of Documents  
U.S. Government Printing Office  
Mail Stop SSOP  
Washington, DC 20402-0001  
Internet: bookstore.gpo.gov  
Telephone: 202-512-1800  
Fax: 202-512-2250
2. The National Technical Information Service  
Springfield, VA 22161-0002  
[www.ntis.gov](http://www.ntis.gov)  
1-800-553-6847 or, locally, 703-605-6000

A single copy of each NRC draft report for comment is available free, to the extent of supply, upon written request as follows:

Address: Office of the Chief Information Officer,  
Reproduction and Distribution  
Services Section  
U.S. Nuclear Regulatory Commission  
Washington, DC 20555-0001  
E-mail: [DISTRIBUTION@nrc.gov](mailto:DISTRIBUTION@nrc.gov)  
Facsimile: 301-415-2289

Some publications in the NUREG series that are posted at NRC's Web site address <http://www.nrc.gov/reading-rm/doc-collections/nuregs> are updated periodically and may differ from the last printed version. Although references to material found on a Web site bear the date the material was accessed, the material available on the date cited may subsequently be removed from the site.

**Non-NRC Reference Material**

Documents available from public and special technical libraries include all open literature items, such as books, journal articles, and transactions, *Federal Register* notices, Federal and State legislation, and congressional reports. Such documents as theses, dissertations, foreign reports and translations, and non-NRC conference proceedings may be purchased from their sponsoring organization.

Copies of industry codes and standards used in a substantive manner in the NRC regulatory process are maintained at—

The NRC Technical Library  
Two White Flint North  
11545 Rockville Pike  
Rockville, MD 20852-2738

These standards are available in the library for reference use by the public. Codes and standards are usually copyrighted and may be purchased from the originating organization or, if they are American National Standards, from—

American National Standards Institute  
11 West 42<sup>nd</sup> Street  
New York, NY 10036-8002  
[www.ansi.org](http://www.ansi.org)

Legally binding regulatory requirements are stated only in laws; NRC regulations; licenses, including technical specifications; or orders, not in NUREG-series publications. The views expressed in contractor-prepared publications in this series are not necessarily those of the NRC.

The NUREG series comprises (1) technical and administrative reports and books prepared by the staff (NUREG-XXXX) or agency contractors (NUREG/CR-XXXX), (2) proceedings of conferences (NUREG/CP-XXXX), (3) reports resulting from international agreements (NUREG/IA-XXXX), (4) brochures (NUREG/BR-XXXX), and (5) compilations of legal decisions and orders of the Commission and Atomic and Safety Licensing Boards and of Directors' decisions under Section 2.206 of NRC's regulations (NUREG-0750).

212-642-4900

**DISCLAIMER:** This report was prepared as an account of work sponsored by an agency of the U.S. Government. Neither the U.S. Government nor any agency thereof, nor any employee, makes any warranty, expressed or implied, or assumes any legal liability or responsibility for any third party's use, or the results of such use, of any information, apparatus, product, or process disclosed in this publication, or represents that its use by such third party would not infringe privately owned rights.

---

---

# **A Combined Analytical Study to Characterize Uranium Soil and Sediment Contamination: The Case of the Naturita UMTRA Site and the Role of Grain Coatings**

---

---

Manuscript Completed: August 2005

Date Published: February 2006

Prepared by

C. F. Jové Colón<sup>1</sup>, C. Sanpawanichakit<sup>2</sup>, H. Xu<sup>3</sup>,  
R.T. Cygan<sup>1</sup>, J.A. Davis<sup>4</sup>, D.M. Meece<sup>4</sup>, R.L. Hervig<sup>5</sup>

<sup>1</sup>Sandia National Laboratories  
Albuquerque, NM 87185-0754

<sup>2</sup>Colorado School of Mines  
Environmental Science and Engineering  
Golden, CO 80401

<sup>3</sup>Department of Earth and Planetary Sciences  
University of New Mexico  
Albuquerque, NM 87131

<sup>4</sup>Water Resources Division  
United States Geological Survey  
345 Middlefield Road  
Menlo Park, CA 94025

<sup>5</sup>Department of Geological Sciences  
Arizona State University  
Tempe, AZ 87287-1404

E. O'Donnell, NRC Project Manager

**Prepared for**  
**Division of Systems Analysis and Regulatory Effectiveness**  
**Office of Nuclear Regulatory Research**  
**U.S. Nuclear Regulatory Commission**  
**Washington, DC 20555-0001**  
**NRC Job Code W6464**





## ABSTRACT

Composite sediment samples from the Uranium Mill Tailings Remedial Action site at Naturita, Colorado were analyzed for uranium using a suite of microbeam analytical techniques encompassing Scanning Electron Microscopy–Energy Dispersive Spectrometry (SEM-EDS), Secondary Ion Mass Spectrometry (SIMS), High Resolution Transmission Electron Microscopy (HRTEM), Micro-Synchrotron X-Ray Fluorescence (M-SXRF), and Micro-X-Ray Absorption Near-Edge Spectroscopy (M-XANES). Two sets of alluvial sediment samples were considered in this study: an untreated composite sediment sampled from several uranium contaminated wells, and a carbonate-free (treated) composite sediment from an area significantly up-gradient from the contaminated portion of the site. The carbonate-free sample was treated with Na-acetate to remove carbonate material and then subsequently exposed to  $10^{-5}$  molal uranyl ( $U^{6+}$ ) nitrate solution. The purpose of the treatment was to investigate uranium adsorption onto the sediment without complications resulting from carbonate complexation with uranyl ions. In all samples, SEM-EDS analysis showed the conspicuous presence of Fe-rich and Al-Si rich (clay) coating layers surrounding the periphery of soil/sediment grains. The bulk grains that serve as substrate to the overlying coatings are mostly quartz and detrital feldspar. The Fe-rich coatings are arranged conformably in both continuous and discontinuous modes, in some cases between the quartz interface and the clay-rich region. However, Fe-rich phases are also present as small scattered particles immersed in the clay layer. SIMS analysis on polished epoxy grain mounts of the naturally-contaminated composite sample reveals the presence of uranium diffusely distributed within the Al-Si rich clay layer. No clear association between Fe and uranium from materials collected in sampling wells with the highest level of uranium contamination was discerned using this analytical technique. However, M-SXRF analyses on the laboratory contaminated carbonate-free sample reveals a close association between uranium and Fe-rich domains on the grain surface. HRTEM analysis on a single grain from the carbonate-free sample characterized by this strong uranium-Fe spatial correlation indicate that these Fe-bearing phases are highly heterogeneous, composed mainly of mixed domains of hematite, goethite, and nanoporous and/or amorphous Fe-(oxy)hydroxides. These Fe-rich nanoporous and amorphous domains within larger Fe-bearing grains are identified as ferrihydrite on the basis of HRTEM observations. The arrangement of Fe-rich amorphous phase domains along with crystalline goethite resembles aggregated textural forms. However, HRTEM analysis indicates that these domains are structurally coherent and continuous, suggesting homogeneous transformation. Mixed layer illite/smectite (I/S) clays are to a great extent the main coating phases present hosting nanosized Fe and Ti oxides. On the basis of these combined analytical observations, mixed layer clays and Fe-rich coatings are the main sinks for uranium in the composite sediment material at Naturita.

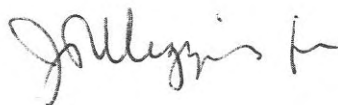


## FOREWORD

This contractor technical report was prepared by Sandia National Laboratories under their Interagency Work Order with the U.S. Nuclear Regulatory Commission, in collaboration with the Colorado School of Mines, University of New Mexico, U.S. Geological Survey, and Arizona State University. An amended version has been submitted to the journal *Geochimica et Cosmochimica Acta* for peer review and publication.

This report summarizes the results of a task to characterize uranium contamination on sediment samples from the UMTRA waste site at Naturita, Colorado. For the characterization, a suite of sophisticated instrumental analysis methods, including electron microscopies, ion microprobe, and synchrotron-based methods, was used to determine the presence and concentration of uranium in the micron-scale surface coatings associated with the bulk weathered soil and sediment aggregates. Standard analytical techniques such as X-ray diffraction and other bulk methods are not sensitive enough to discriminate the surface material from the bulk phases. The results of the characterization suggest that clay and iron-rich coatings are the primary locations for uranium at Naturita. Identification of the substrate hosting the contamination is important in the application of surface complexation models in performance assessment studies particularly in dynamic systems where flow rates permit access to adsorption sites in coatings but not to the interior of bulk phases. Although a suite of sophisticated analytical methods was needed to determine the location of the adsorbed uranium in the Naturita samples, the complete suite may not be necessary at a typical field site. At those sites optical microscopy and one or two of the above methods may be sufficient to identify the coatings and bulk matrix materials, and this information could be used to build an appropriate surface complexation model. The significant result from a regulatory perspective is that mineral coatings cannot be ignored and may, in fact, be the primary controlling mechanism for adsorption.

The views and opinions presented in this report are those of the individual authors, and publication of this report does not necessarily constitute NRC approval or agreement with the information contained herein. As such, this report is not a substitute for NRC regulations. The approaches and methods described are provided for information only, and compliance is not required. Moreover, use of product or trade names herein is for identification purposes only and does not constitute endorsement by the NRC or Sandia National Laboratories.



---

Carl J. Paperiello, Director  
Office of Nuclear Regulatory Research  
U.S. Nuclear Regulatory Commission





# CONTENTS

	<u>Page</u>
<b>Abstract</b> .....	iii
<b>Foreword</b> .....	v
<b>Executive Summary</b> .....	xi
<b>Abbreviations</b> .....	xiii
<b>Acknowledgements</b> .....	xv
<b>1. Introduction</b> .....	1-1
<b>2. Naturita Site Characteristics</b> .....	2-1
<b>3. Sample Description</b> .....	3-1
<b>4. Analytical Methods and Results</b> .....	4-1
4.1 Scanning Electron Microscopy with Energy Dispersive Spectroscopy.....	4-1
4.2 Secondary Ion Mass Spectrometry .....	4-7
4.3 High Resolution Transmission Electron Microscopy .....	4-7
4.4 Micro Synchrotron X-Ray Florescence and Micro X-Ray Absorption Near-Edge Spectroscopy .....	4-8
<b>5. Conclusions</b> .....	5-1
<b>6. References</b> .....	6-1



## Figures

	<b>Page</b>
1. Naturita sampling well site map redrawn after Davis et al. (1999) .....	3-2
2. Combined Back-Scattered Electron Image (BSEI) and corresponding SEM-EDS elemental maps for sample MAU-04 .....	4-2
3. SIMS elemental maps for sample MAU-04 .....	4-5
4. HRTEM images showing typical illite/smectite clay submicroscopic textures found in the composite Naturita alluvial samples .....	4-10
5. Low-magnification, bright-field TEM image of the carbonate-free sample (509.18 grain aggregate).....	4-11
6. TEM image of the uranium-treated carbonate-free sample (509.18) showing two goethite crystals .....	4-13
7. High-resolution TEM image of uranium-treated carbonate-free sample and inverse transform of FFT image .....	4-16
8. Schematic diagram of the X-26A beamline for M-SXRF analysis at BNL NSLS.....	4-16
9. U(L $\alpha_1$ ) and Fe (K $\alpha$ ) maps of uranium-treated sample 509.18 UNC-COMP sample ....	4-17
10. Fe(K $\alpha$ ) and Zn(K $\alpha$ ) maps of uranium-treated sample 509.18 UNC-COMP sample.....	4-18
11. M-XANES spectra spot analysis on uranium-treated sample 509.18 UNC-COMP compared to uranium standards .....	4-19



## EXECUTIVE SUMMARY

This contractor technical report was prepared by Sandia National Laboratories (SNL) under their Interagency Work Order (JCN W6811 and JCN Y6464) with the U.S. Nuclear Regulatory Commission. This report summarizes the results of a task to characterize uranium adsorption at a remediated uranium mill tailings site in Naturita, Colorado which has been under study by the U.S. Geological Survey (USGS) for several years. A suite of surface analytical techniques was used to investigate the role of micron-scale grain coatings in uranium adsorption under varying chemical conditions. The result of this investigation gives insights into the potential sites for metal adsorption onto various soil/sediment minerals. The information on mechanisms controlling adsorption reported here is being applied by SNL to enhance the prediction of radionuclide transport through soil and sediment. The expected outcome will make regulatory decision-making more realistic.

The research described in this report is part of a larger effort being sponsored by NRC's Office of Nuclear Regulatory Research (RES) to systematically address the problem of model conservatism and uncertainty in predictive environmental models. The traditional approach of constant distribution coefficients ( $K_D$  approach) is an oversimplification requiring uniform environments and constant conditions (in time and space) that are not realistic representations of the natural environment. The traditional batch experiments used for  $K_D$  measurements extract a number that is an average of the effect of many processes but holds only for those specific conditions under which it was measured. As a result, distribution coefficients often vary by many orders of magnitude and are only valid at the point of measurement and for the conditions measured. The  $K_D$  approach works best for contaminants that adsorb weakly to soil and aquifer sediments, are present in low concentration, participate in few reactions, and occur in a groundwater system where chemical conditions such as contaminant concentration and pH vary little. Most heavy metals and many of the cationic radionuclides, however, adsorb rather strongly to a variety of surfaces, especially the oxyhydroxides and transition metals, and many of the cations react to form various species and complexes. As a result, the  $K_D$  approach cannot be expected to describe adsorption effectively for these two important classes of contaminants.

It is important to address possible alternatives to the  $K_D$  approach because in many cases the  $K_D$ -based transport models give results that are not only quantitatively inaccurate, but qualitatively wrong. The  $K_D$ -based models greatly overestimate plume advance, understate the difficulty in removing contaminants from the subsurface, and fail to anticipate a "tail" of contamination in discharge from the contaminated zone that persists indefinitely. These inaccuracies are sufficient to lead (in the absence of other overriding factors, such as past experience) to (1) poor design in environmental remediation or monitoring projects, or (2) reliance on performance estimates for regulatory decisions that may underestimate the consequences of those decisions.

RES has been working through SNL and the USGS to assess alternatives to the  $K_D$  approach with the intent of developing a credible scientific basis for a computationally efficient, yet realistic, approach to modeling adsorption processes at the field scale. The SNL project is addressing the basic mechanisms controlling adsorption. SNL's research integrates the results of fundamental theory and experiments with field measurements to better understand the complex nature of adsorption of radionuclides onto mineral surfaces and provides a sound theoretical basis for the assumptions and parameter values of the surface complexation models

developed by the USGS. SNL has taken a multidisciplinary approach, which integrates the results of fundamental theory and experiments with field measurements to better understand the complex nature of adsorption of radionuclides. This NUREG/CR report is one part of that effort. It is part of a cooperative effort with the USGS at Naturita, Colorado to assess radionuclide transport in the environment at a complex field site.

The SNL and USGS research has successfully accounted for the uranium migration at the Naturita site (see related publications referenced in this report). Further work will be necessary to extend that approach to other radionuclides and to account for other environmental conditions.

## ABBREVIATIONS

BNL	Brookhaven National Laboratory
BSEI	Back-Scattered Electron Image
EDS	Energy Dispersive Spectroscopy
FFT	Fast Fourier Transform
HRTEM	High Resolution Transmission Electron Microscopy
I/S	illite/smectite
LLW	Low Level Waste
M-SXRF	Micro-Synchrotron X-Ray Fluorescence
M-XANES	Micro-X-Ray Absorption Near-Edge Spectroscopy
NSLS	National Synchrotron Light Source
SAED	Selected Area Electron Diffraction
SEM-EDS	Scanning Electron Microscopy-Energy Dispersive Spectrometry
SIMS	Secondary Ion Mass Spectrometry
SNL	Sandia National Laboratories
SPI	Structure Probe, Inc.
TEM	Transmission Electron Microscopy
U	uranium
UO <sub>2</sub> <sup>2+</sup>	uranyl ion
UMTRA	Uranium Mill Tailings Remedial Action
UNC-COMP	uncontaminated composite
XRD	X-Ray Diffraction





## **ACKNOWLEDGEMENTS**

The authors are grateful for the financial support of the United States Nuclear Regulatory Commission and the valuable assistance provided by the project manager Edward O'Donnell during the course of this study. The authors are also indebted to Antonio Lanzirroti and William Rao (Brookhaven National Laboratory, NSLS Beamline X-26A), Pengchu Zhang (Sandia National Laboratories), Paul Hlava (Sandia National Laboratories), Bruce Honeyman (Colorado School of Mines), Stephen Sutton (University of Chicago, CARS consortium), Howard Anderson (Sandia National Laboratories), and Alice Kilgo (Sandia National Laboratories) for their very helpful assistance in providing support for the analyses and sample preparation presented in this study. Patrick Brady and Henry Westrich provided valuable reviews of the original manuscript that greatly benefited the final article. SNL is a multi-program laboratory operated by the Sandia Corporation, a Lockheed Martin Company, for the United States Department of Energy under Contract DE-AC04-94AL85000.



# 1. INTRODUCTION

Mineral surfaces in soil and sediment phases often serve as sinks for many complex engineered contaminants whether organic or inorganic. Soils and/or shallow alluvial sedimentary deposits are inherently heterogeneous in nature, encompassing a large suite of organic and inorganic phases which may interact with fluids in the matrix. These interactions often form surface coatings on the mineral grains of the soil and sediments which can significantly modify the overall surface properties of the substrate mineral (Coston et al., 1995; Davis, 1982; Davis, 2001; Jenne, 1998; Jové Colón et al., 2001). These coatings, which usually have a different identity from the mineral substrate, can serve as efficient adsorption sites for metal ions. Coatings often have a much higher adsorption capacity than the substrate itself. The most common ones are micron to nanometer sized phases of clay, goethite, and ferrihydrite and the coating is a very small percent of the bulk volume of soil/sediment particles, often less than 5%. Because coatings make up only a small percent of the total volume of the material they are often overlooked in bulk chemical or mineralogical analyses made by optical methods, X-ray diffraction, or X-ray fluorescence.

Grain coatings and the associated growth textures have been widely studied in porous sedimentary rocks (e.g., Ehrenberg, 1993; Hurst and Nadeau, 1995) but to a lesser degree in natural soil material (e.g., Barker and Banfield, 1996; Coston et al., 1995; Padmanabhan and Mermut, 1996; Zachara et al., 1995). The primary emphasis on consolidated sedimentary materials is due to the effect of mineral coatings on groundwater flow properties (e.g., porosity and permeability) (Aagaard et al., 2000; Hurst and Nadeau, 1995; Nadeau and Hurst, 1991). Occlusion of connecting pores and throat channels due to formation of secondary minerals are, to a significant extent, strongly dependent upon the growth textures and habits of authigenic or secondary phases (Aagaard et al., 2000; Ehrenberg, 1993). Conversely, in some cases, diagenetic mineral coatings such as chlorite have an important role in preserving sandstone porosity (Aagaard et al., 2000; Ehrenberg, 1993). Therefore, mineral coatings in porous sedimentary formations exemplify their importance in modifying the overall physical properties of the bulk rock. Similarly, coatings can significantly modify surface properties of the mineral such as surface charge thus potentially effecting metal sorption and transport in the porous media (Hendershot and Lavkulich, 1983; Barber et al. 1992; Fuller et al., 1996; Knapp et al., 1998; Gabriel et al., 1998). This study attempts to delineate the important role of surface grain coatings in soil/sediment minerals serving as efficient sinks of radionuclide pollutants in the subsurface environment. Furthermore, the application and implementation of radionuclide adsorption into reactive-transport models to predict or estimate field-scale contaminant mobility necessitates comprehensive information on the primary sinks for contaminant uptake at mineral surfaces (Davis et al., 2000; Davis and Curtis, 2003; 2005; Waite et al., 1994).

This report addresses the identification and characterization of the minerals that control uranium sorption at the Naturita, Colorado Uranium Mill Tailings Remedial Action Project (UMTRA) site. The Naturita site was chosen because it was well characterized by the U.S. Geological Survey (USGS) in their investigation of the application of surface complexation modeling methodology for assessment of uranium transport in groundwater, and the Survey provided the sediment samples used in this study. Uranium was extracted from the Naturita site for several decades starting in the late 1940s (see e.g., the website for the UMTRA Groundwater Project; UMTRA, 2002a; see also Section 2). These activities resulted in the accumulation of large quantities of residual mill tailings exposed to the open atmosphere and therefore vulnerable to meteoric processes such as rain, wind, and snow melt (White et al., 1984). These processes mobilized

some of the uranium in the tailings and it was leached into an adjacent near-surface aquifer. A similar mode of contamination is not only observed at UMTRA sites, but in other nuclear material processing facilities (see Czyscinski et al., 1982) where low level nuclear waste (LLW) was deposited or buried at relatively shallow depths.

The research is part of a larger cooperative project to develop information for providing more realistic models for assessing radionuclide transport in the environment. The overall project involves the USGS, the U.S. Nuclear Regulatory Commission (NRC), Sandia National Laboratories (SNL), and Southwest Research Institute's Center for Nuclear Waste Regulatory Analysis (CNWRA). Sandia's role in the overall study involves integration of the results of fundamental theory and experiments with field measurements to better understand the complex nature of sorption of radionuclides onto mineral surfaces. This report addresses one part of that effort and it deals with a characterization of uranium sorption onto soil/sediment particles to determine what role the particle, the particle coating, and the matrix of soil/sediment aggregates play in uranium sorption at the Naturita site. Other components of Sandia's research include column experiments (Westrich et al., 1998), synchrotron-based microtomography for determining the relationships of adsorption sites in alluvial soils to iron and pore space distributions in soils particles (McLain et al., 2002; Altman et al. 2005), uncertainty analysis in reactive transport modeling (Criscenti et al., 2002), and molecular modeling of adsorption processes (Teter and Cygan, 2002).

The present study concentrates on the direct observation of uranium on contaminated sediment material from the Naturita site utilizing microbeam analytical spectroscopic techniques. Contrary to previous studies that indirectly assessed the identity of surface coating in the grain matrix components (e.g., mechanical separation; Zachara, et al., 1995), this study approaches the characterization of mineral coatings by direct observation of the hosting grain substrate. Therefore, the present approach allows for a more realistic observation of the spatial, compositional, and structural relationships between coating and substrate. To assess the mineralogy and location of sorption sites in the Naturita alluvial material, a suite of analytical techniques were used including: Scanning Electron Microscopy–Energy Dispersive Spectrometry (SEM-EDS), Secondary Ion Mass Spectrometry (SIMS), High Resolution Transmission Electron Microscopy (HRTEM), Micro-Synchrotron X-Ray Fluorescence (M-SXRF), and Micro-X-Ray Absorption Near-Edge Spectroscopy. Two kinds of samples were investigated: (1) a composite sediment sampled from several uranium contaminated wells, and a carbonate-free (treated) composite sediment sample from an area significantly up-gradient from the contaminated portion of the site. The carbonate-free sample was treated with Na-acetate to remove carbonate material and then subsequently exposed to  $10^{-5}$  molal uranyl ( $U^{6+}$ ) nitrate solution. The purpose of the treatment was to investigate uranium sorption on the collected material without complications resulting from carbonate complexation with uranyl ions. The results from this study of the role of grain coatings in uranium adsorption at Naturita will be an important input into reactive-transport models which can be used for estimation of field-scale contaminant transport.

## 2. NATURITA SITE CHATACTERISTICS

The Naturita site is one of the 24 United States Department of Energy UMTRA sites where the mill tailings were removed and disposed elsewhere, but still left a legacy of contaminated soil, shallow alluvium, and groundwater aquifers. The Naturita site is situated on floodplain alluvial sediments close to the San Miguel River in the southwestern Colorado county of Montrose (Figure 1; Davis et al., 1999; Davis et al., 2000; Davis and Curtis, 2005). According to the UMTRA Groundwater Project (UMTRA, 2002b), the Naturita site hosted approximately 418,000 cubic meters of contaminated tailings that underwent chemical extraction. Uranium ore extractions at UMTRA sites were typically performed through sulfuric acid leaching methods (UMTRA, 2002c). The estimated volume of contaminated water is in the neighborhood of 380,000 m<sup>3</sup> (UMTRA, 2002b). The approximate surface area of comprising contamination is approximately 10<sup>6</sup> m<sup>2</sup> (UMTRA, 2002d).

A monitoring network of groundwater wells cover almost the entire contamination site. Some are capable of performing single- and multilevel sampling of the shallow alluvial aquifer (Davis et al., 2000). Recently, the United States Geological Survey conducted extensive hydrological and water sampling activities, including the incorporation of new sampling wells to expand the existing hydrological monitoring network within the site. Specific details on the field hydrological monitoring and the subsequent results are documented in reports by Davis et al. (1999; 2000) and Davis and Curtis (2005).



### 3. SAMPLE DESCRIPTION

The Naturita site is adjacent to the San Miguel River and is underlain by floodplain-type sediments. The average annual precipitation is approximately 23 cm (9 inches) per year. According to the Web Soil Survey data from the U.S. Department of Agriculture ([websoilsurvey.nrcs.usda.gov/app/WebSoilSurvey.aspx](http://websoilsurvey.nrcs.usda.gov/app/WebSoilSurvey.aspx)) for the area corresponding to the Naturita site, the main type of soils mapped at the site in the vicinity of the San Miguel river are referred as fluvaquents (see Soil Survey Staff, 1999). Two kinds of samples were incorporated in this analytical study: 1) an uncontaminated composite sample (UNC-COMP) sampled obtained upstream from the contaminated area which was treated for carbonate removal, and subsequently exposed to an uranyl ( $U^{6+}$  as  $UO_2^{2+}$ ) solution, and 2) an untreated contaminated composite sample taken from the most contaminated wells (MAU-4 and NAT-06) in the site (see Figure 1). The removal of carbonate from the first group of samples was incorporated to investigate uranium sorption on the soil without complications resulting from carbonate complexation with uranyl ions. In general, the composite samples are comprised mostly of quartz with lesser amounts of detrital feldspar, carbonates, and fine clay material. The clay fraction is highly variable, ranging mostly from intricate mixed-layer illite/smectite (I/S) clays to the minor presence of chlorite. Magnetic separation of the soil samples revealed a non-negligible fraction of magnetite, indicating the ubiquitous presence of Fe oxides. Subordinate amounts of barite and gypsum can be found sporadically filling cavities and crevices in larger grains.

As noted previously, the treated samples were obtained near the San Miguel River up-gradient from the contaminated area (see Figure 1). Carbonate was removed by using a Na-acetate solution. Following this treatment, the carbonate-free samples were exposed to  $10^{-5}$  molal uranyl nitrate solution. This artificially-contaminated sample was mounted with epoxy to a petrographic glass slide. Naturally contaminated samples were not treated prior to analysis. Naturally-(untreated) and artificially-(treated) contaminated samples were also mounted in cylindrical epoxy with a diameter and thickness of 2.5 cm (1 inch). These grain mounts were carefully polished on one face, using standard sequential grinding and polishing materials, to preserve the fine coating surrounding larger substrate grains and aggregated composite textures.

# Naturita Site Sampling Well Map

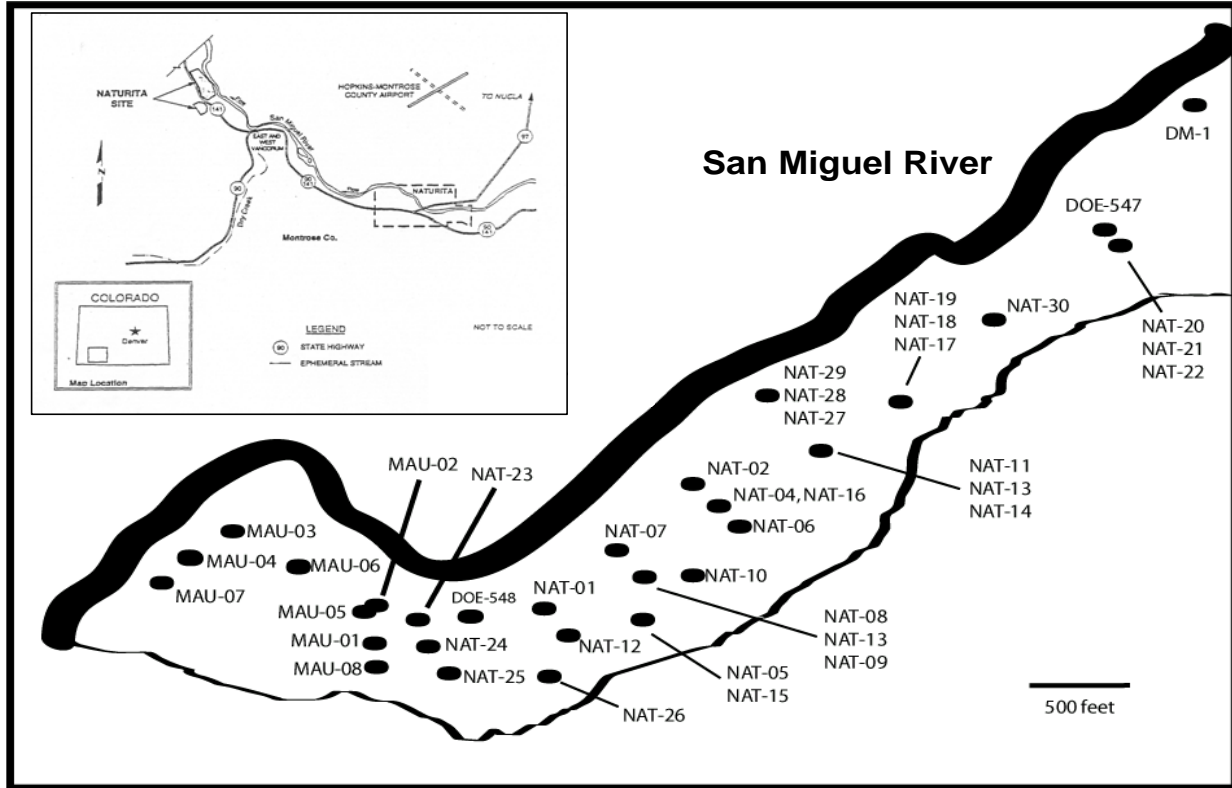


Figure 1. Naturita sampling well site map redrawn after Davis et al. (1999). The map excludes the wells immediately adjacent to the San Miguel River.



## 4. ANALYTICAL METHODS AND RESULTS

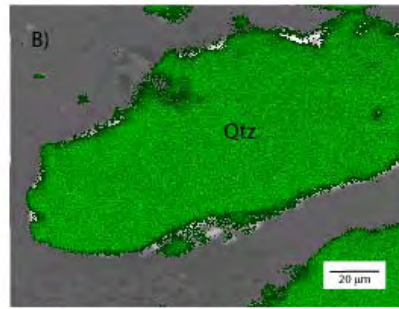
Various analytical techniques were used in this study encompassing bulk analysis by X-Ray Diffraction (XRD) and the combined use of microbeam and spectroscopic techniques capable of (1) identifying the coating phase, (2) showing fine-scale structural features of the coating phase, and (3) compositional mapping of elemental constituents which can be related to the fine scale features of the coating phase. These microbeam techniques include Scanning Electron Microscopy with Energy Dispersive Spectrometry (SEM-EDS), Secondary Ion Mass Spectrometry (SIMS), High Resolution Transmission Electron Microscopy (HRTEM), Micro Synchrotron X-Ray Fluorescence (M-SXRF), and Micro X-Ray Absorption Near-Edge Spectroscopy (M-XANES). Although no single analytical method fully characterizes the uranium-bearing mineral coating, the combination of techniques provides a detailed view of uranium content and spatial distribution, mineral identity and crystallinity, and other mineral associations.

### 4.1 Scanning Electron Microscopy with Energy Dispersive Spectroscopy

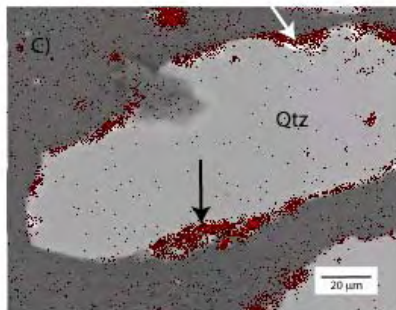
SEM-EDS was used to obtain qualitative elemental maps of selected sample grains on polished epoxy grain mounts. The analyses were conducted on a JEOL JSM-T300 SEM housed in the facilities of the Geochemistry Department, Sandia National Laboratories (SNL). The SEM is equipped with a Kevex EDS unit using iXRF Systems (Houston, Texas) software and interfacing components for performing point analyses, line scan profiles, and multi-element maps. The working conditions for the SEM include an accelerating voltage of 15–20 kV and a beam current of 5 mA. SEM-EDS analyses were conducted on the flat-polished epoxy grain mounts. Count accumulation times in the generation of elemental maps ranged from 4 to 10 seconds for each scanning step, depending on the size of analyzed area. This initial approach established the spatial definition of grain coatings in the sampled granular material. For this analysis, the epoxy-mounted grains were coated with a thin carbon layer using an Structure Probe, Inc. (SPI) carbon coater. Elemental maps and line scans were generally targeted to analyze medium or sand-size grains (mainly quartz) with a long-axis dimension of 80–100 micrometers. Elemental maps of quartz grains of this approximate size revealed the best preservation of grain coatings within the elemental detection scale. The optimized scanning conditions also revealed coating thickness ranging from ~10 to ~15 micrometers. Figures 2a and 2b depict representative elemental maps on quartz grains from the samples naturally contaminated by the uranium plume. Notice in the photomicrographs for sample MAU-04 the conspicuous presence Al- and Fe-rich rims surrounding the substrate quartz grains. These rim coatings can be nearly continuous or irregular around the grain periphery. The coating commonly covers grain surface irregularities like valleys and gaps in a continuous fashion. Figure 2c shows typical soil aggregate textures composed of a heterogeneous mixture of detrital grains held together mainly by clays. These aggregates have “porous” textures with gaping spaces between grain boundaries that could serve as fast diffusion pathways when in contact with aqueous fluids. Based on the elemental mappings of the quartz grains and the aggregates, the Al-rich Si-deficient rims are interpreted as thin clay coatings. In some cases, some Fe-rich areas (with no observable Si) are spatially situated at the clay-quartz interface (Figure 2a, panel E). Uranium was below detection limits of the Energy Dispersive Spectroscopy (EDS) technique; therefore, no spatial elemental mapping was assessed using this analytical technique.



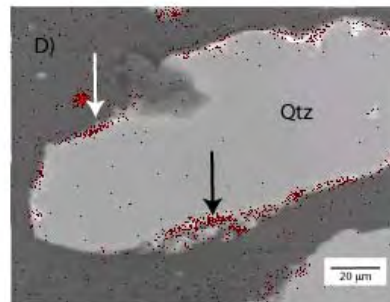
Back-Scattered Electron Image (BSEI) of a quartz grain in sample from well MAU-04. The grayscale gradients at the grain rim delineate the presence of a different phase.



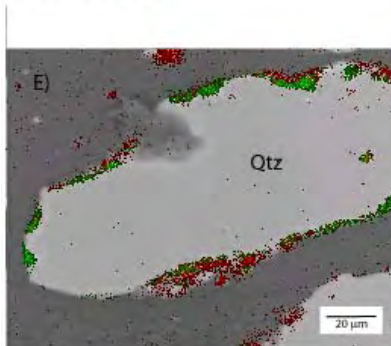
Combined BSEI and X-ray map of Si (green) of this grain identified as quartz. Notice the relatively lower abundance of Si at the grain rim.



Combined BSEI and X-ray map of Al (red). Al possibly delineates predominant amounts of clay (arrows) present at the grain rim area.

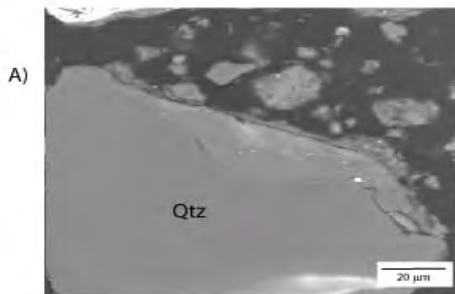


Combined BSEI and X-ray map of K (red). The apparent correlation of K and Al delineates the possible presence of an outer clay (arrows) bordering the quartz grain.

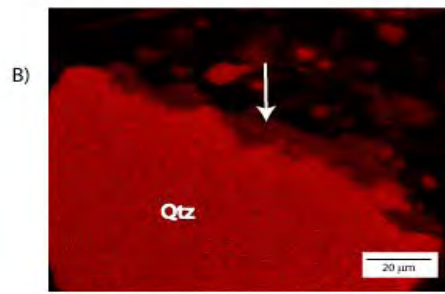


Combined X-ray map of Al (red) and Fe (green). Notice the presence of Fe (probably as an oxo-hydroxide) underlying the Al (Clay?) rim.

**Figure 2a.** Panels A through E show the combined Back-Scattered Electron Image (BSEI) and corresponding SEM-EDS elemental maps (see labels) for sample MAU-4 from the contaminated area. Notice the well-defined Si-Al coating surrounding the quartz grain substrate.



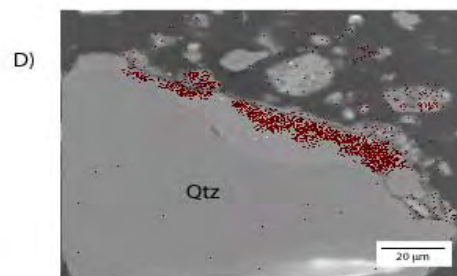
Back-Scattered Electron Image (BSEI) of a quartz grain. The grayscale gradients within and at the grain rim delineate the presence of a different phase or an overgrowth.



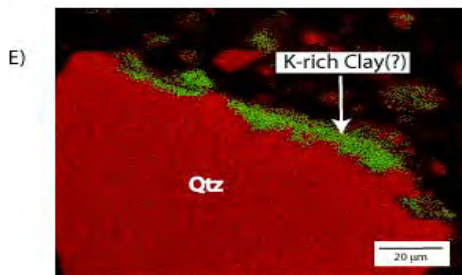
X-ray map of Si (red). Notice the relatively lower abundance of Si at the grain rim (arrow).



Combined BSEI and X-ray map of Al (green). Al possibly delineates predominant amounts of clay (arrows) present at the grain rim area.

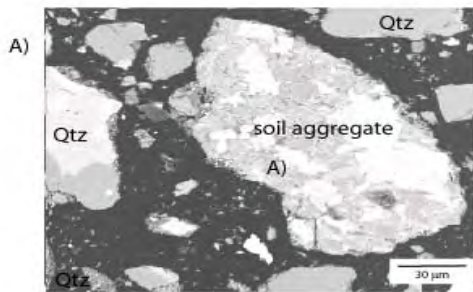


Combined BSEI and X-ray map of K (red). The good correlation between K and Al suggests the presence of a K-rich clay armoring the larger quartz grain.

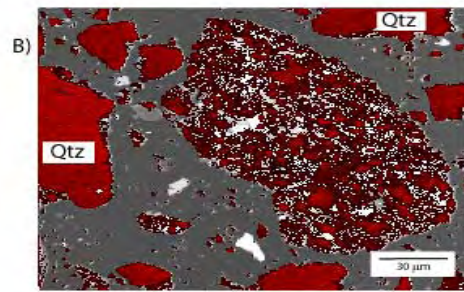


Combined X-ray map of Al (green) and Si (red) to better depict the relative location of clay(?) and quartz. This phase distribution is typical for της Νατυριτα σοιλ.

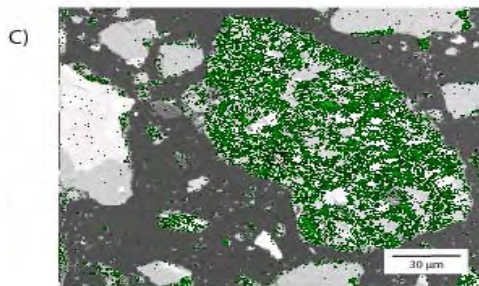
**Figure 2b.** Panels A through E show the combined BSEI and corresponding SEM-EDS elemental maps for sample MAU-04 from the contaminated area (see labels). Notice how the suspected clay-rich coating fills rough surface irregularities on the quartz grain.



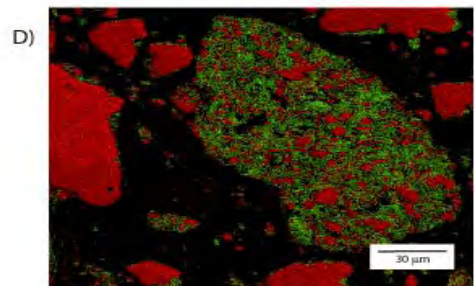
Back-Scattered Electron Image (BSEI) of soil aggregate in sample from well MAU-04. The grayscale gradients at the grain rim delineate the presence of a different phase.



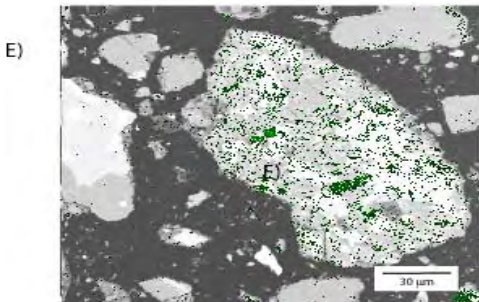
Combined BSEI and X-ray map of Si (red). The Si patches in the large aggregate grain likely represent a combination of quartz and clay grains. Quartz (qtz) grains are identified around the aggregate.



Combined BSEI and X-ray map of Al (green). Al could be used to trace predominant amounts of clay present as grains or grain coatings.

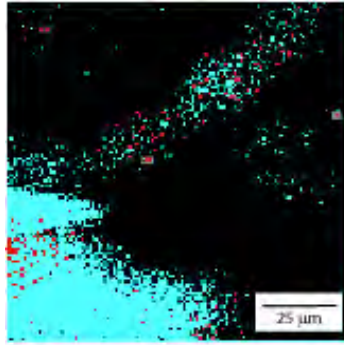


Combined X-ray map of Al (green) and Si (red). Notice the presence of Al around quartz rims (upper right-hand corner) depicting a grain coating.

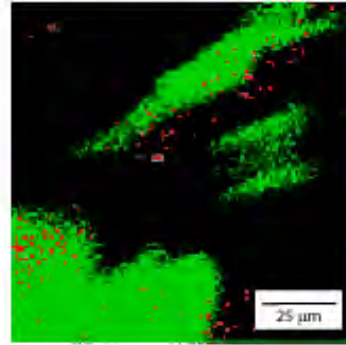


Combined BSEI and X-ray map of K (green). K seems to be highly disseminated within the aggregate but is sometimes concentrated within minor phases.

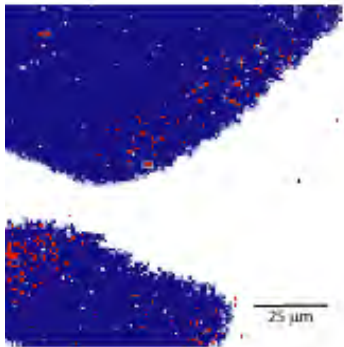
**Figure 2c.** Panels A through E show the combined BSEI and corresponding SEM-EDS elemental maps for sample MAU-04 from the contaminated area (see labels). Notice the heterogeneous nature of the aggregate and its relatively large microporosity due to composite texture.



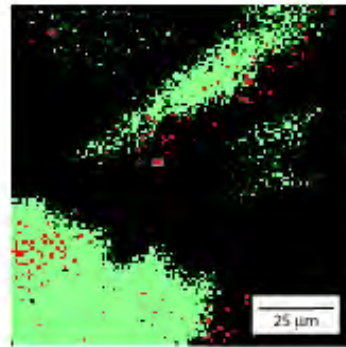
MAU-04 ( $^{27}\text{Al}$ )



MAU-04 ( $^{39}\text{K}$ )



MAU-04 ( $^{28}\text{Si}$ )



MAU-04 ( $^{56}\text{Fe}$ )

**Figure 3a. SIMS elemental maps for sample MAU-04 from the contaminated area.  $^{235}\text{U}$  is shown as a red dot overlay in each panel. Notice the strong spatial correlation of  $^{235}\text{U}$ ,  $^{28}\text{Si}$ , and  $^{27}\text{Al}$  maps, suggesting a strong association with a clay-rich coating in the outer boundaries of the grain. Color contrast in the pixels was enhanced to intensify the color difference in the elemental map. Grain boundaries are denoted by the  $^{28}\text{Si}$  map; no optical image is available for this technique.**

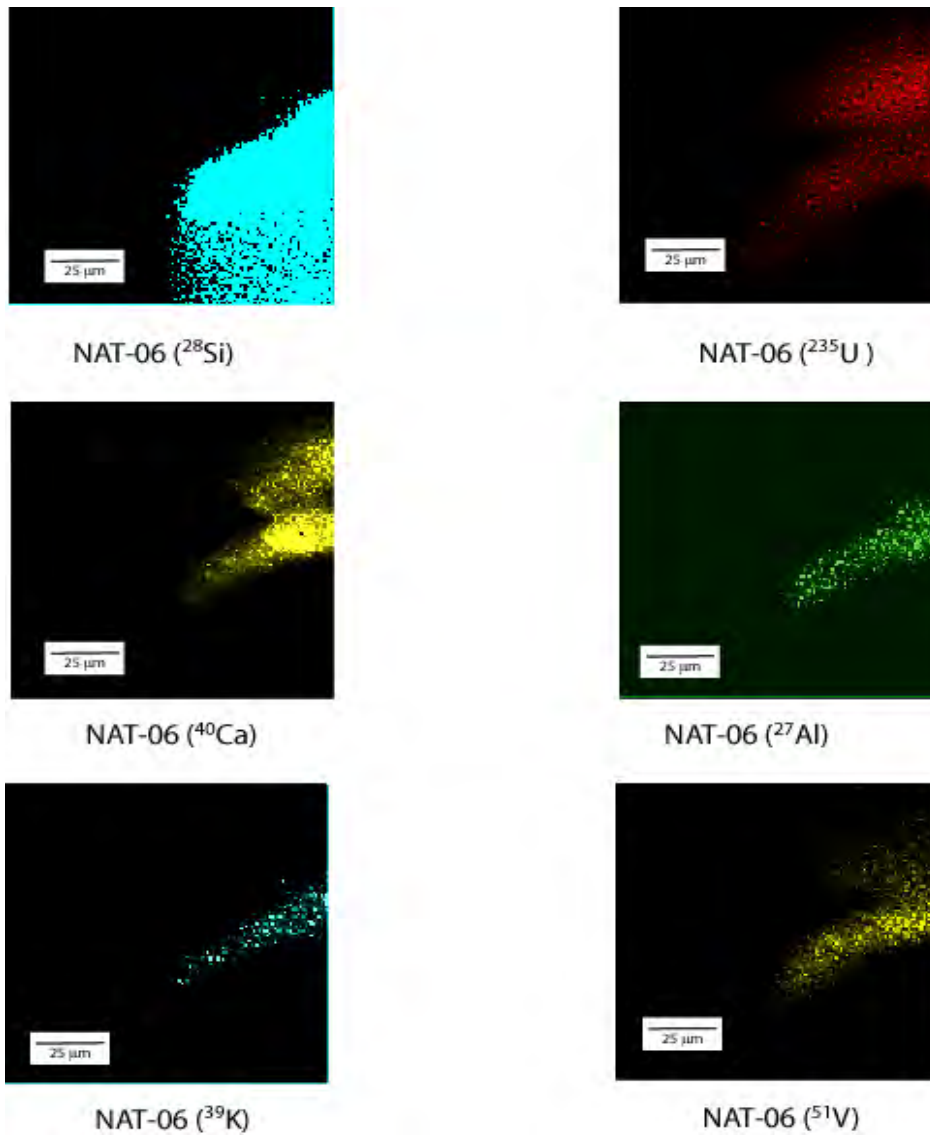


**Figure 3b. SIMS elemental maps for sample NAT-06 from the contaminated area. Notice the strong spatial correlation of  $^{235}\text{U}$  and,  $^{28}\text{Si}$ ,  $^{40}\text{Ca}$ ,  $^{39}\text{K}$ ,  $^{51}\text{V}$ , and  $^{27}\text{Al}$ . Note that the  $^{40}\text{Ca}$  'patch-like' spot correlates well with  $^{235}\text{U}$ . Because of the absence of other elements, it is inferred that this Ca-rich domain may be a carbonate domain coexisting with a clay coating.  $^{235}\text{U}$  map also indicates a strong association with a clay-rich coating in the outer boundaries of the grain. Color contrast in the pixels was enhanced to intensify the difference in the elemental map.**

## **4.2 Secondary Ion Mass Spectrometry**

SIMS analyses were conducted on a CAMECA IMS 3f instrument at the Arizona State University SIMS Laboratory in Tempe, Arizona. The primary sputtering  $O^-$  ionic beam was set to beam currents of up to 100 nanoamps to measure uranium. The accelerating voltage of secondary ions with a positive charge was 4.5 kV. The secondary ion signal was maximized using aperture sizes of 400 and 1800 microns for contrast and field, respectively. The primary beam residence time during the rasterizing procedure was sufficiently large (i.e., relative to the time of flight of the ions) that analysis did not require time-of-flight corrections. Image rasterizing of secondary ions was achieved through instrument modifications allowing for spatial control of the primary beam onto the sample. Data acquisition of the secondary ion signal and conversion to pixel images was attained using a commercial software package from Emispec, Inc. (Tempe, Arizona). Beam current was adjusted until enough uranium counts were obtained to discern scans on an average collection times of 65 millisecond/pixel in a average coverage area of 123 x 123 pixel frame. Lower counting times (i.e., faster scans) were used during initial exploratory reconnaissance of uranium in one-dimensional (line) and two-dimensional (frame) scans in multiple grains conducted from the edges towards the grain interior. Two-dimensional frame scans typically covered an approximate area of ~100 square microns. As in the SEM-EDS analyses, the samples analyzed by SIMS are flat-polished epoxy grain mounts. Figures 3a and 3b show elemental maps of  $^{27}Al$ ,  $^{28}Si$ ,  $^{40}Ca$ ,  $^{56}Fe$ ,  $^{39}K$ , and  $^{238}U$ . A comparison between  $^{238}U$  and other elemental maps indicates that uranium is spatially associated with a Si-Al rich layer. The homogeneous  $^{28}Si$  map in both samples indicates that the substrate grains are quartz, as confirmed by complementary methods, such as SEM-EDS, for the bulk mineral composition of the composite sample. The elemental maps also show that the Al-rich rims, for which the  $^{238}U$  dot map conforms, are up to ~10 microns thick. Further, the  $^{238}U$  map shows that its spatial distribution roughly covers the area delineated by the  $^{27}Al$  map. This observation suggests that uranium diffuses deep within the clay coating in the naturally-contaminated samples. Unfortunately, continuous Fe-rich coatings of reasonably detectable thickness were not observed when using SIMS for the studied samples to establish a similar relationship with U. The only spatial association with  $^{56}Fe$  is seen on a suspected clay coating, as depicted in Figure 3a. The SIMS analytical technique proved to be spatially and compositionally sensitive within the scale of the grain coatings and substrates. However, the analytical setup did not allow for unequivocal identification of the analyzed grain as discerned by SEM-EDS, where coupling of morphological and compositional observations aid in the textural bulk characterization of grain coatings, as well as the substrate grain. Therefore, substrate and coating identity were inferred from the elemental compositional distributions obtained with the SIMS scans. Figure 3b show a “cloud” of a uranium-rich zone spatially on top of the  $^{28}Si$  and  $^{27}Al$  layer but overlapping the region delineated by  $^{40}Ca$ . This  $^{40}Ca$ -rich area may be a coexisting carbonate coating with the clay. Similar textural relations in coatings have been observed by SEM-EDS and HRTEM. Relative to these other analytical methods, SIMS and the ion microprobe are complementary but provide a superior sensitivity in the analysis of uranium.

## **4.3 High Resolution Transmission Electron Microscopy**

Characterization of coating material for the Naturita samples at the nano- and micronscale was performed at the Department of Earth and Planetary Sciences, University of New Mexico (Albuquerque, New Mexico) using a state-of-the-art JEOL 2010 HRTEM and JEOL-2010F STEM fitted with an Oxford Instruments Link ISIS EDS system. HRTEM analyses were conducted at an accelerating voltage of 200 KeV and a point-to-point resolution of 0.19 nm.

Beam diameter in the EDS analyses ranged from about 10 nm to 100 nm, depending on the spot analysis. The HRTEM technique reveals submicron interfacial relations and structural characterization of coatings and grain substrates. Two types of sample preparation were used prior to the analysis: ion-milled, sand-sized grains and fine-grained segregated granular fractions obtained from the bulk samples. The naturally-contaminated NAT-06 and MAU-4 and the carbonate-free treated UNC-COMP samples show an intricate suite of clay phases, composed mostly of interlayered illite/smectite present as coatings and/or as separate phases (Figures 4a and 4b). Some extraneous nanosized phases are immersed in the main clay coat that includes rutile (TiO<sub>2</sub>), quartz, and well- and poorly-crystallized (or nanoporous) Fe-(oxy)hydroxides like hematite, goethite, and ferrihydrite (Figures 5a, 5b, and 5c). Various examples of these Fe-hydroxides show goethite and ferrihydrite closely coexisting in distinct domains (Figures 6a, 6b, and 6c). Goethite domains are dominant with ferrihydrite domains in these crystals being less common. The mixed or intergrown domains of goethite and ferrihydrite occur with significant nanopores and pitted surfaces suggesting a greater ability to adsorb uranium. Interlayered illite/smectite dominate the clay coating material in the observed bulk of selected grains, but kaolinite is also observed (Figure 5d). The compositional range of the illite/smectite clays is  $K_{0.14-0.50}Ca_{0.09-0.20}(Al_{1.41-2.07}Fe_{0.11-0.59}Mg_{0.06-0.75})(Si_{3.25-3.58}Al_{0.30-0.75})_4(OH)_2 \cdot nH_2O$  as determined by EDS methods. Less abundant carbonate material, such as calcite, is also present in the coatings and appears to coexist with clays and Fe-oxide phases.

The uranium-treated carbonate-free sample was analyzed in both bulk samples and in a specific grain aggregate (referred hereafter as sample 509.18) that were also analyzed by M-SXRF. This specific grain was removed from the epoxy mount and analyzed by HRTEM without undergoing sample preparation (e.g., ion milling). Calcite particles were not detected in this particular sample. HRTEM analysis of both bulk and grain aggregate 509.18 also reveals an apparent larger population of poorly crystalline Fe-(oxy)hydroxide phases forming intricate coatings with nanoporous textural domains within bigger Fe-bearing phases (Figures 6a, 6b, and 6c). The cryptocrystalline and nanoporous nature of the coatings suggests that these aggregate-like phases contain a large surface area that plausibly serves as a preferential site for uranium adsorption. These aggregate-like textures in the Fe-bearing coatings phases bear a resemblance to those reported by Banfield et al. (2000) for bio-mediated growth of Fe-(oxy)hydroxides. However, HRTEM reveals that there are intimate textural relations between goethite and ferrihydrite domains which indicate a complex combination of distinct nanoporous domains related in a structurally coherent and continuous fashion, rather than distinct nanocrystalline domains, as implied by aggregated-based growth (see Figure 7a and 7b). A possible explanation is that the Fe-rich particle contains areas of ferrihydrite homogeneously transforming to the more crystalline goethite phase, a feature also observed by Banfield et al. (2000) in their study of nanoscale Fe-rich aggregates.

#### **4.4 Micro Synchrotron X-Ray Fluorescence and Micro X-Ray Absorption Near-Edge Spectroscopy**

M-SXRF and M-XANES analyses were conducted at Brookhaven National Laboratory (BNL) National Synchrotron Light Source (NSLS) beamline X-26A. This particular beamline was dedicated to the use of M-SXRF to investigate the spatial quantification of minor elements in geological materials (Bertsch and Hunter, 2001). Figure 8 shows a schematic diagram illustrating the M-SXRF configuration at beamline X-26A. An excellent review on the technique and the multiple applications of synchrotron microbeam analysis to the earth sciences is given by Bertsch and Hunter (2001).



Several aggregated grain samples from Naturita were surveyed for U(L $\alpha_1$ ), Fe(K $\alpha$ ), Zn(K $\alpha$ ), Rb(K $\alpha$ ), Ti(K $\alpha$ ), and V(K $\alpha$ ) using M-SXRF through elemental maps and line scans. However, only the uranium-treated carbonate-free sample clearly revealed detectable uranium in distinct domain areas of  $\sim 1 \text{ mm}^2$ . Therefore, this particular sample was selected for the M-SXRF analyses presented in this study. The 509.18 sample is comprised of several fine-sized grains cemented together with a matrix of intergranular material. M-SXRF elemental maps shown in Figures 9 and 10 for the aggregate grains in the treated carbonate-free material (originally derived from UNC-COMP sample) depict the multi-element distribution frames for uranium and Fe. Figure 9 elemental maps indicate an evident spatial correlation between Fe and uranium for the carbonate-free sample. This correlation conforms with Fe-rich areas, but some smaller regions situated in the central regions of the grain do not correlate as well. Because of the spectral limitations from instrument settings needed to detect uranium at the time of the analysis,

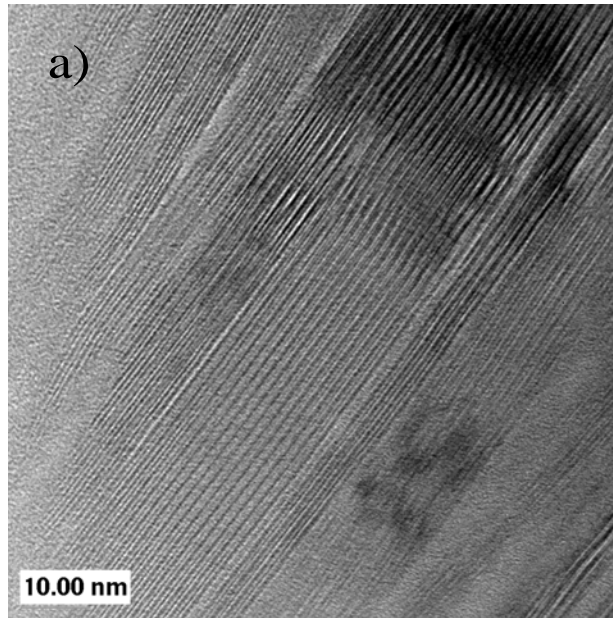


**Figure 4a.** HRTEM image showing typical illite/smectite clay submicroscopic textures found in the composite Naturita alluvial samples (UNC-COMP shown here).

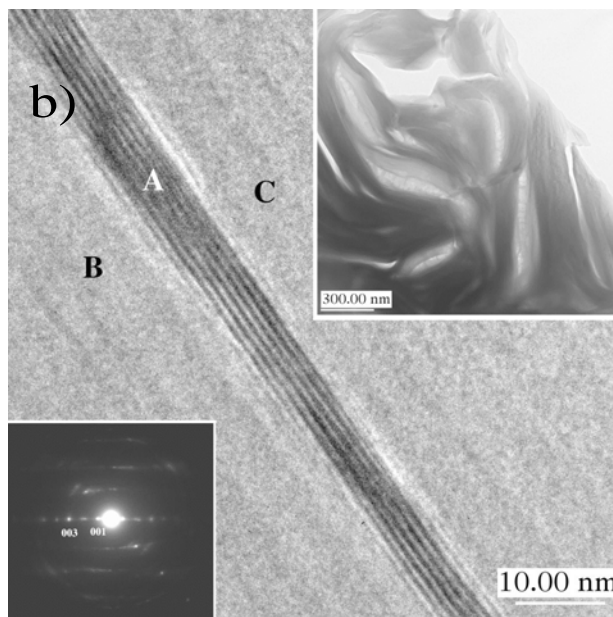


**Figure 4b.** Transmission Electron Microscopy (TEM) image of the carbonate-free sample showing an illite/smectite crystal (A) along (001). The clays on the two sides of the crystal (A) are also illite/smectite clays in an off-zone axis orientation. The lower left corner shows the selected area electron diffraction (SAED) pattern indicating the illite/smectite has  $1M_d$  polytype structure. Low magnification TEM image (upper right corner) shows a contorted texture of the clay phase.

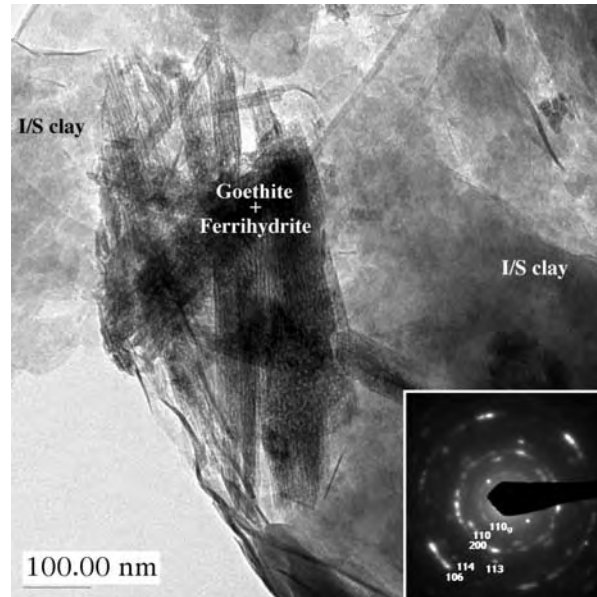


Figure 5a. Low-magnification, bright-field TEM image of the carbonate-free sample (509.18 grain aggregate; see text) showing plate-like ferrihydrite immersed in illite/smectite clay. The lower right corner shows the electron diffraction pattern for ferrihydrite. A weak diffraction labeled as  $110_g$  indicates the presence of small amount of goethite in the predominant ferrihydrite phase.

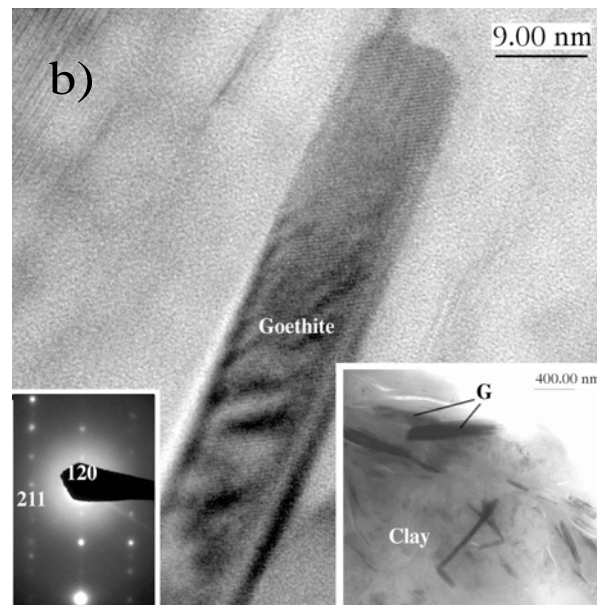
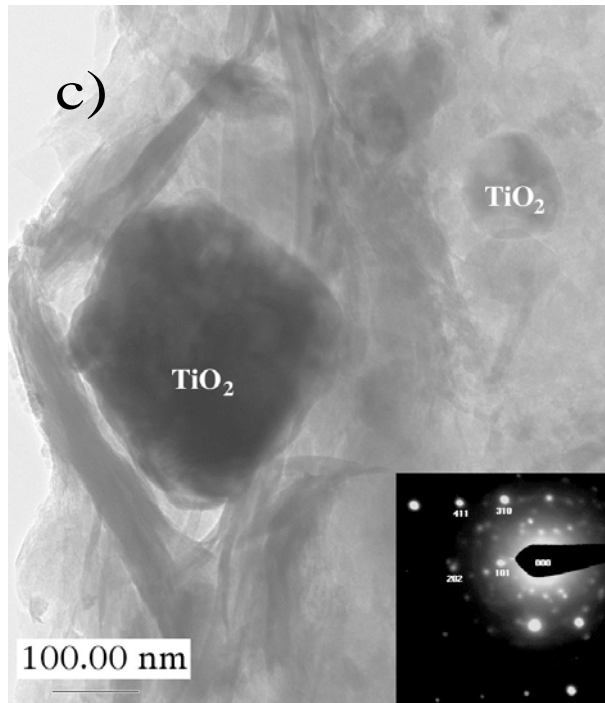
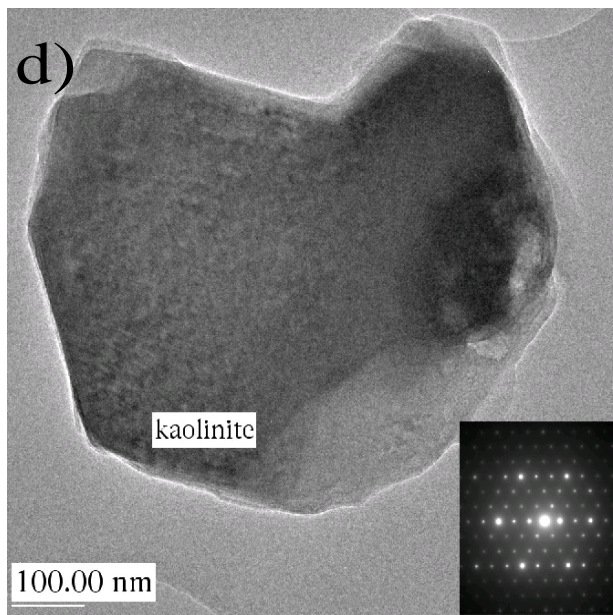


Figure 5b. Bright-field TEM images of the 509.18 sample showing needle-like goethite crystals immersed in illite/smectite clay matrix. Inserted is the SAED pattern (lower left corner) of the needle-like goethite crystal at the center of the high magnification image. Low magnification TEM image showing many goethite (G) needles (lower right corner).



**Figure 5c.** Low magnification TEM image showing rutile ( $\text{TiO}_2$ ) crystals immersed in the illite/smectite clay matrix of the carbonate-free sample. The lower right corner shows a SAED pattern from the large rutile grain.



**Figure 5d.** Low magnification TEM image showing a kaolinite crystal of the carbonate-free sample. The lower right corner shows the SAED pattern.

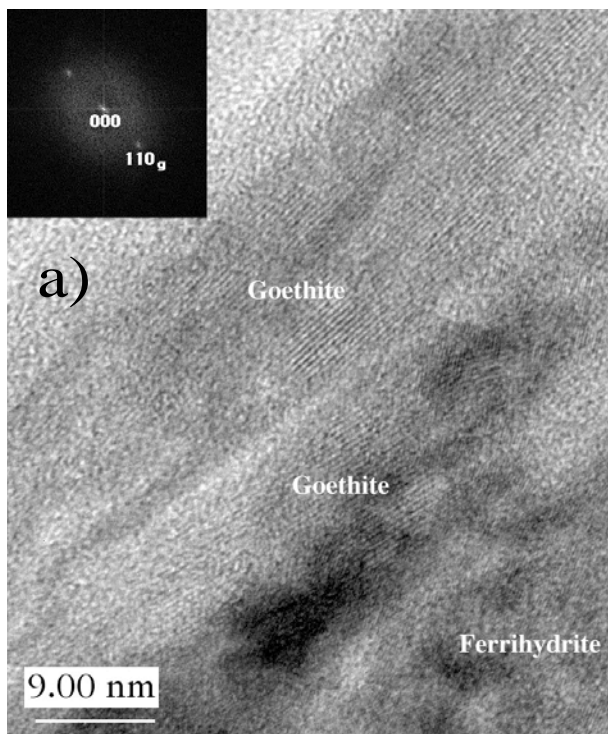


Figure 6a. TEM image of the uranium-treated carbonate-free sample (509.18) showing two goethite crystals with low-angle boundary between them coexisting with ferrihydrite.

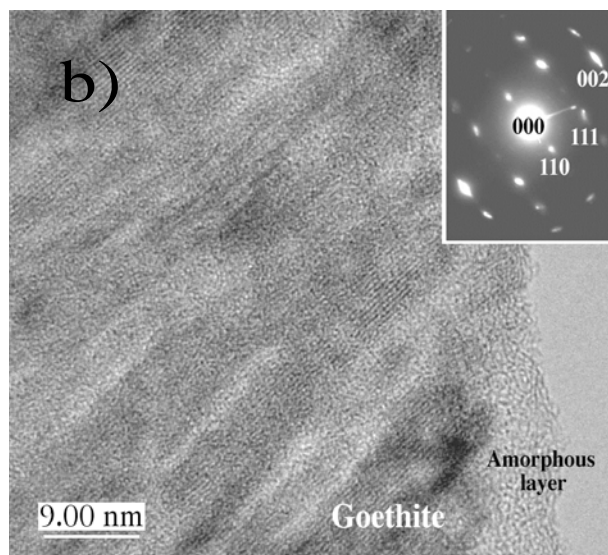
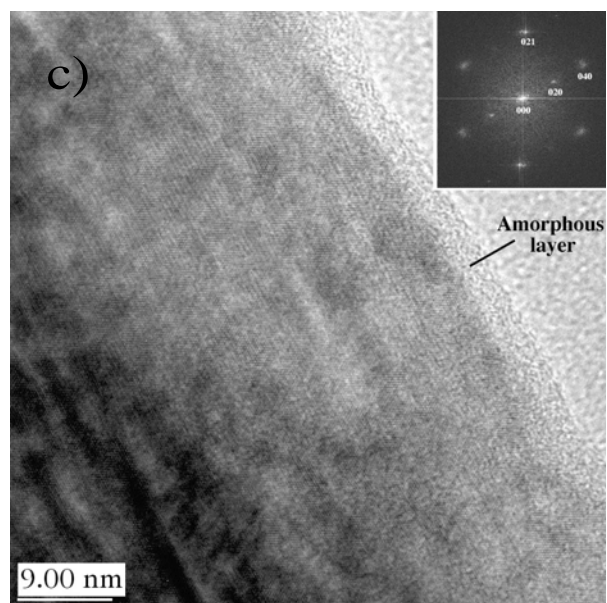


Figure 6b. TEM image of the uranium-treated carbonate-free sample (sample 509.18) showing goethite crystal domains with similar orientations and amorphous-like Fe-hydroxide on the surface between goethite domains. Inserted is the SAED pattern (upper right corner) from this “poorly crystalline” goethite.



**Figure 6c. High-resolution TEM image of the uranium-treated carbonate-free sample showing crystalline (coherent) domains of ferrihydrite and goethite. The top right corner is a Fast Fourier Transform from the image showing a relatively sharp (020) reflection from goethite only. Other diffuse reflections characterize the poorly crystalline nature (or small crystal domains) in the ferrihydrite matrix. The crystal has an amorphous-like layer on the surface.**

M-SXRF could not detect other elements of relevance in coating characterization, such as Al and Si. However, SEM-EDS analysis on the same sample 509.18 suggest that the surface also contains Al. The substrate grain was identified as quartz based on Si elemental mapping. HRTEM analysis on the same grain also reveals the presence of kaolinite (Figure 7d). It could be inferred that clays play a significant role in uranium uptake but it is evident that Fe-rich phases (identified as a combination Fe-(oxy)hydroxides) are the main sink for uranium in this carbonate-free sample. Another strong correlation was found between Fe and Zn for grain 509.18. Figure 10 shows two elemental maps for Fe and Zn depicting a good spatial correspondence even when the relative number of counts for Zn is smaller. Coston et al. (1995) reports  $Pb^{2+}$  and  $Zn^{2+}$  adsorption experiments onto Al-Fe coatings in sandy material from an aquifer. The authors concluded that adsorption of both species was controlled by the coatings on the quartz grains found in the aquifer. Based on the adsorption experiments, Coston et al. (1995) concluded that  $Zn^{2+}$  uptake was favored over  $Pb^{2+}$  by Al-rich surface sites. Direct M-SXRF observations on spatial Zn-Fe associations suggest that  $Zn^{2+}$  could have strong affinities to Fe-rich phases, but further studies are needed on this aspect.

M-XANES analyses were focused on an area in sample 509.18 which was rich in Fe and where a relatively large number of uranium counts were also detected. Figure 11 show the resulting spectra, along with a video snapshot delineating the analyzed surface region in grain 509.18. In Figure 11, the combined spectra of the  $UO_2(U^{6+})$  and  $UO_3(U^{4+})$  standards indicate that the local redox state of uranium in the Fe-rich domain is in the hexavalent form  $U^{6+}$ . This was assessed by examining the absorption edge position relative to uranium oxide standards in the XANES

spectra, as featured by the major absorption peak displaced towards the higher energy side of the spectra, indicative of  $U^{6+}$  (Bertsch and Hunter, 2001).

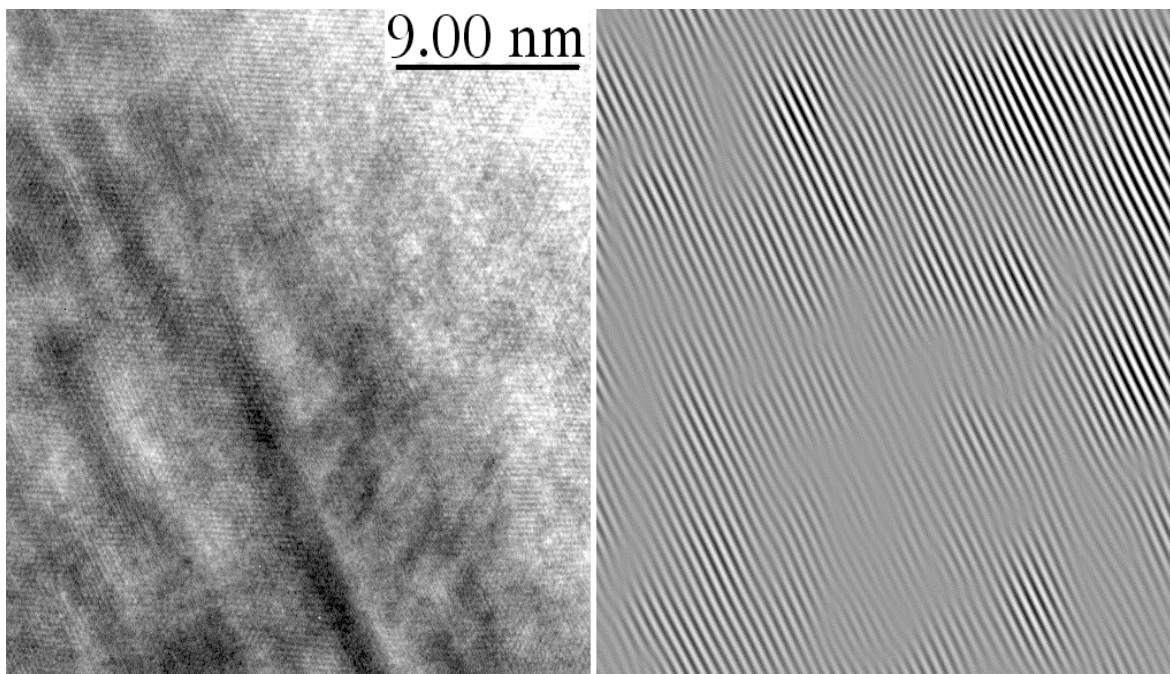


Figure 7. Left: High-resolution TEM image from lower-left corner of Figure 6c. Areas of goethite domains show 5 Å (020) fringes. Right: Inverse Fourier transform of a FFT from left image (like the one inserted in Figure 6c using only the (020) reflection and showing lattice fringes of goethite only). Notice the irregular shape of the goethite areas and ferrihydrite domains between them.

X26 A Microprobe Beamline

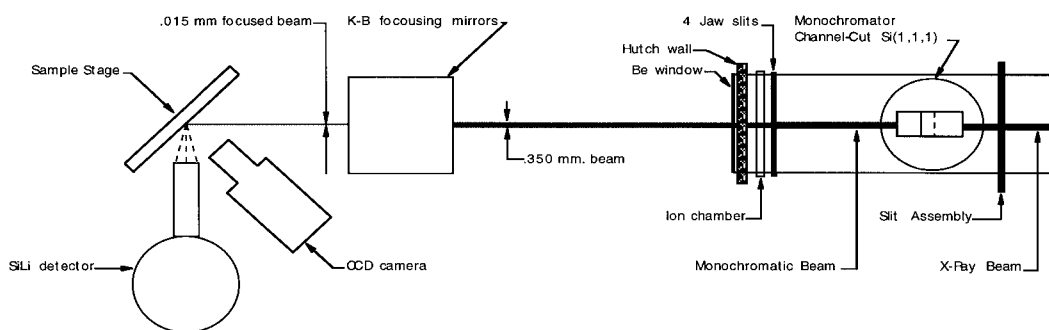
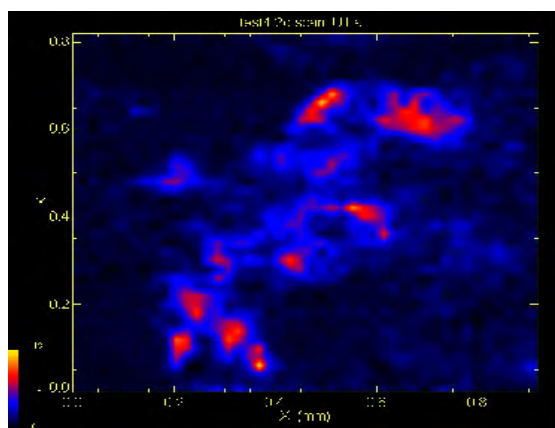


Figure 8. Schematic diagram of the X-26A beamline for M-SXRF analysis at Brookhaven National Laboratory National Synchrotron Light Source (diagram courtesy of William Rao and Antonio Lanzirroti, BNL NSLS).

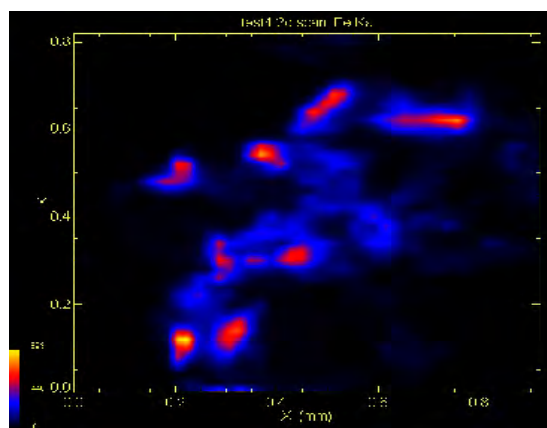




Optical view



U(L $\alpha_1$ )

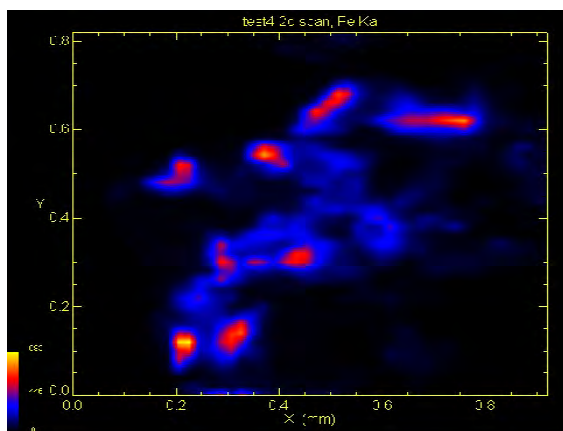


Fe(K  $\alpha$ )

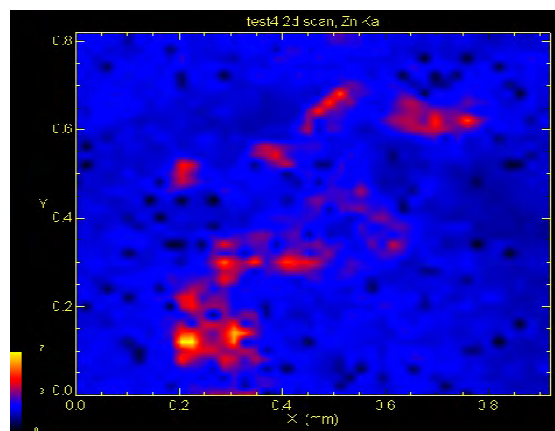
**Figure 9. U(L $\alpha_1$ ) and Fe (K $\alpha$ ) maps of uranium-treated sample 509.18 UNC-COMP sample. Optical image was obtained from a video view of the sample with a scale similar to that of the elemental maps. Intensity bar scale represents counts. Notice the close spatial correspondence between both elements.**



Optical view



Fe(K  $\alpha$ )



Zn(K  $\alpha$ )

**Figure 10. Fe(K $\alpha$ ) and Zn(K $\alpha$ ) maps of uranium-treated sample 509.18 UNC-COMP. Optical view and scale are similar to that of the elemental maps. Intensity bar scale represents counts (see text).**

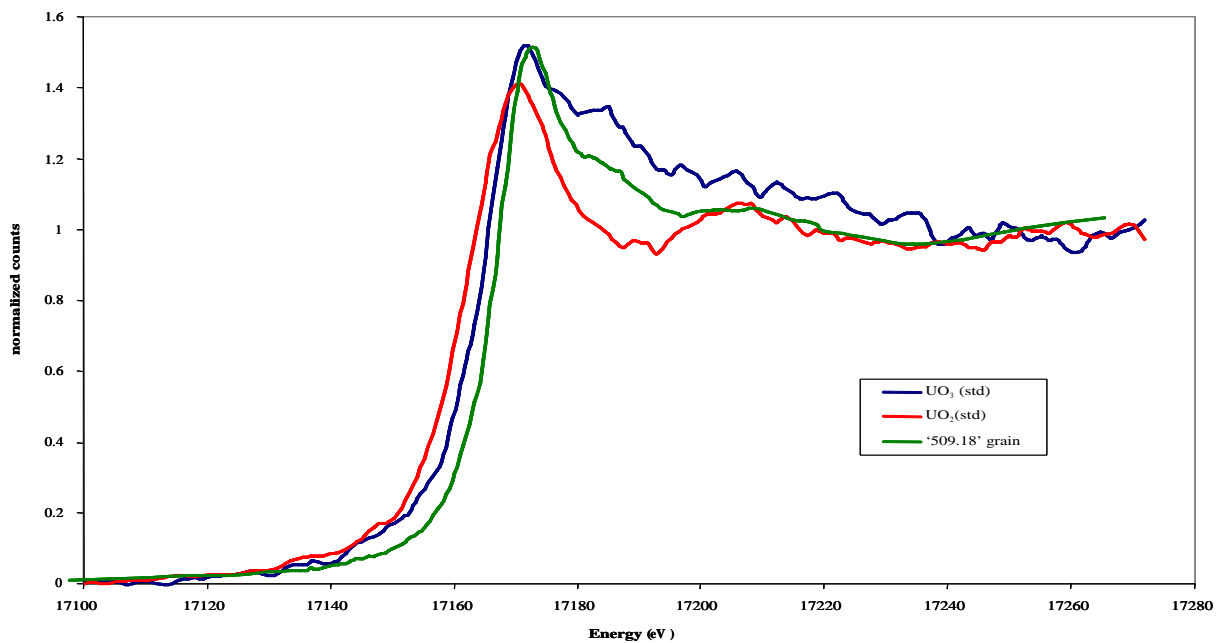
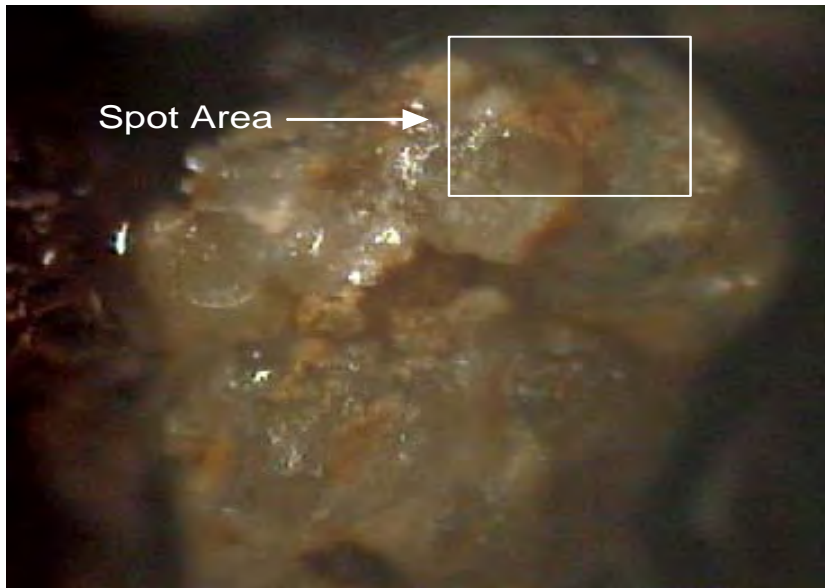


Figure 11. M-XANES spectra spot analysis on uranium-treated sample 509.18 UNC-COMP compared to  $U^{4+}O_2(s)$  and  $U^{6+}O_3(s)$  standards. The shift of the absorption edge peak position to a higher energy indicates that the local redox state of uranium in this Fe-rich area is in the hexavalent state ( $U^{6+}$ ).

## 5. CONCLUSIONS

The microscopic characterization of the Naturita soil/sediment material delineated above indicates that uranium sorption sites are located in micron scale coatings of the particles. The coatings are mainly combined interlayered illite/smectite clays and Fe-(oxy)hydroxides including ferrihydrite and goethite. Uranium is restricted to the grain coatings and perhaps grain boundaries, and does not exceed a thickness of ~10-15 microns. Uranium was not found inward of the grain coatings, or within the substrate grains. However, aggregates of soil particles may incorporate some uranium within them due to their microporosity and "open" pathways for diffusion from the surrounding interfacial region of the grain. The latter is a topic of further study.

In contrast to previous observations on quartz grains coated with Fe-oxides from oxisols (Padmanabhan and Mermut, 1996) the mineral coatings in the Naturita sediment are rarely arranged concentrically around grains. Rather, they are discontinuous illite/smectite clays irregularly arranged relative to the interface with the quartz substrate. A common observation among various samples was that the illite/smectite clays and kaolinite appear to coexist with Fe-(oxy)hydroxides and, in some cases, with carbonate material. The coexistence between clays and Fe-(oxy)hydroxides was also reported by Padmanabhan and Mermut (1996). Nanoscale observations on the heterogeneous arrangement of Fe-(oxy)hydroxides within Fe-rich particles indicate complex but coexisting domains of cryptocrystalline or amorphous ferrihydrite and crystalline goethite often mimicking aggregate-like textures. HRTEM observations suggest that these heterogeneous domains are structurally coherent and continuous at the nanoscale. This implies a homogeneous transformation process in the coating phase between, for example, an amorphous-like phase such as ferrihydrite to a more crystalline one like goethite, as opposed to the particle aggregation described by Banfield et al. (2000). Indeed, geochemical processes involving particle aggregation associated with colloids at the solid-fluid interface should be quite apparent in soil and shallow alluvial environments, but this study did not reveal evidence of this textural characteristic in most of the examined grain coatings. The nanoporous ferrihydrite material found at Naturita possesses a large surface area that may provide preferential sites for uranium sorption. These processes can have significant consequences on the bulk contaminant uptake properties of the soil/sediment and should be taken into account when developing models entailing adsorption-desorption processes in soils or weathered sediment environments.

This study necessitated the use of a combination of microprobe and spectroscopic techniques to generate the information needed for identification of the compositional and structural characteristics of surface coatings and uranium adsorption sites in the Naturita composite material. This information is also essential for describing radionuclide scavenging and partitioning in the subsurface environment and for revealing the identity of major uranium getters or sinks at the mineral surface. The results of this study will aid in the implementation of quantitative surface adsorption approaches in reactive-transport models used to predict and develop scenarios present in field-scale contamination applications.



## 6. REFERENCES

- Aagaard P., Jahren J. S., Harstad A. O., Nilsen O., and Ramm M. (2000) "Formation of grain-coating chlorite in sandstones: Laboratory synthesized vs. natural occurrences." *Clay Minerals* **35**, 261-269.
- Altman, S.J., Rivers, M.L., Reno, M., Cygan, R.T., and McLain, A.A. (2005) "Characterization of sorption sites on aggregate soil samples using synchrotron X-ray computerized microtomography." *Environmental Science and Technology* **39**, 2679-2685.
- Banfield J. F., Welch S. A., Zhang H. Z., Ebert T. T., and Penn R. L. (2000) "Aggregation-based crystal growth and microstructure development in natural iron oxyhydroxide biomineralization products." *Science* **289**(No. 5480), 751-754.
- Barber, L.B., Thurman, E.M., and Runnells, D.D. (1992) "Geochemical heterogeneity in a sand and gravel aquifer: Effect of sediment mineralogy and particle size on the sorption of chlorobenzenes" *Journal of Contaminant Hydrology* **9**, 35-54.
- Barker W. W. and Banfield J. F. (1996) "Biologically versus inorganically mediated weathering reactions: Relationships between minerals and extracellular microbial polymers in lithobiotic communities." *Chemical Geology* **132**(No. 1-4), 55-69.
- Bertsch P. M. and Hunter D. B. (2001) "Applications of synchrotron-based X-ray microprobes." *Chemical Reviews* **101**, 1809-1842.
- Coston J. A., Fuller C. C., and Davis J. A. (1995) "Pb<sup>2+</sup> and Zn<sup>2+</sup> adsorption by a natural aluminum- and iron-bearing surface coating on an aquifer sand." *Geochimica et Cosmochimica Acta* **59**(No. 17), 3535-3547.
- Criscenti, L.J., Eliassi, M., Cygan, R.T., and Jové Colón, C.F. (2002) *Effects of adsorption constant uncertainty on contaminant plume migration: One- and two-dimensional numerical studies*. U.S. Nuclear Regulatory Commission, NUREG/CR-6780.
- Czycinski K. S., Pietrzak R., and Weiss A. J. (1982) *Evaluation of isotope migration - land burial: water chemistry at commercially operated low-level radioactive waste disposal sites*. U.S. Nuclear Regulatory Commission, NUREG/CR-2124.
- Davis J. A. (1982) "Adsorption of natural dissolved organic matter at the oxide/water interface." *Geochimica et Cosmochimica Acta* **46**, 2381-2393.
- Davis J. A. (2001) *Surface complexation modeling of uranium(VI) adsorption on natural assemblages*. U.S. Nuclear Regulatory Commission, NUREG/CR-6708.
- Davis, J. A. and Curtis, G. P. (2005) *Consideration of geochemical issues in groundwater restoration at uranium in-situ leach mining facilities*. U.S. Nuclear Regulatory Commission, NUREG/CR-6870.

Davis J. A., Curtis G. P., and Naftz, D. L. (1999) *Characterization of the Naturita, Colorado field site and field sampling*. U.S. Nuclear Regulatory Commission Letter Report, November 30, 1999.

Davis J. A., Curtis G. P., and Naftz D. L. (2000) *Field demonstration of surface complexation models of sorption at a U.S. remediation site*. U.S. Nuclear Regulatory Commission Letter Report, October 31, 2000.

Davis, J.A. and Curtis, G.P. (2003) *Application of surface complexation modeling to describe uranium(VI) adsorption and retardation at the uranium mill tailings site at Naturita, Colorado*, U.S. Nuclear Regulatory Commission, NUREG CR-6820.

Ehrenberg S. N. (1993) "Preservation of anomalously high porosity in deeply buried sandstones by grain-coating chlorite: examples from the Norwegian continental shelf." *American Association of Petroleum Geologists Bulletin* **77** (No. 7), 1260-1286.

Fuller, C.C., Davis, J.A., Coston, J.A., and Dixon, E. (1996) "Characterization of metal adsorption variability in a sand and gravel aquifer, Cape Cod, Massachusetts, U.S.A." *Journal of Contaminant Hydrology* **22**, 165-187.

Gabriel, U., Gaudet, J.-P., Spadini, L., and Charlet, L. (1998) "Reactive transport of uranyl in a goethite column: an experimental and modelling study" *Chemical Geology* **151**, 107-128.

Hendershot, W.H. and Lavkulich, L.M. (1983) "Effect of sesquioxide coatings on surface charge of standard mineral and soil samples" *Soil Science Society of America Journal*, **47** (No. 6), 1252-1260.

Hurst A. and Nadeau P. H. (1995) "Clay microporosity in reservoir sandstones: An application of quantitative electron microscopy in petrophysical evaluation." *American Association of Petroleum Geologists (AAPG)* **79** (No. 4), 563-573.

Jenne E. A. (1998) "Adsorption of metals by geomedia: Data analysis, modeling, controlling factors, and related issues." In *Adsorption of Metals by Geomedia* (ed. E. A. Jenne), pp. 1-73. Academic Press.

Jové Colón C. F., Brady P. V., Siegel M. D., and Lindgren E. R. (2001) "Historical case analysis of uranium plume attenuation." *Soil and Sediment Contamination* **10**, 71-115.

Knapp, E.P, Herman, J.S., Hornberger, and G.M., Mills, A.L. (1998) "The effect of distribution of iron-oxyhydroxide grain coatings on the transport of bacterial cells in porous media." *Environmental Geology* **33** (No. 4), 243-248.

McLain, A.A., Altman, S.J., Rivers, M.L., and Cygan, R.T. (2002) *Use of computerized microtomography to examine the relationship of sorption sites in alluvial soils to iron and pore space distributions*. U.S. Nuclear Regulatory Commission, NUREG/CR-6784.

Nadeau P. H. and Hurst A. (1991) "Application of back-scattered electron microscopy to the quantification of clay mineral microporosity in sandstones." *Journal of Sedimentary Petrology* **61** (No. 6), 921-925.

Padmanabhan E. and Mermut A. R. (1996) "Submicroscopic structure of Fe-coatings on quartz grains in tropical environments." *Clays and Clay Minerals* **44** (No. 6), 801-810.

Soil Survey Staff (1999) *Soil Taxonomy. Second Edition*. NRCS-USDA Agric. Handb. 436 U.S. Gov. Print. Office.

Teter, D.M. and Cygan, R.T. (2002) *Large-scale molecular dynamics simulations of metal sorption onto the basal surfaces of clay minerals*. U.S. Nuclear Regulatory Commission, NUREG/CR-6757.

UMTRA (2002a) [www.gjo.doe.gov/ugw](http://www.gjo.doe.gov/ugw).

UMTRA (2002b) [www.gjo.doe.gov/ugw/sites/co/naturita/naturita.htm](http://www.gjo.doe.gov/ugw/sites/co/naturita/naturita.htm).

UMTRA (2002c) [www.gjo.doe.gov/ugw/references/factshts.htm](http://www.gjo.doe.gov/ugw/references/factshts.htm).

UMTRA (2002d) [www.gjo.doe.gov/ugw/sites/co/naturita/naturita.htm](http://www.gjo.doe.gov/ugw/sites/co/naturita/naturita.htm).

Waite, T.D., Davis, J. A., Payne, T. E., Waychunas, G. A. and Xu, N. (1994) "Uranium(VI) adsorption to ferrihydrite: Application of a surface complexation model," *Geochimica et Cosmochimica Acta* **58** (No. 24) 5465-5478.

Westrich, H.R., Brady, P.V., Cygan, R.T., Gruenhagen, S.E., Nagy, K.L., and Anderson, H.L. (1998) *Characterization of retardation mechanisms in soil*. U.S. Nuclear Regulatory Commission, NUREG/CR-6603.

White A. F., Delany J. M., Narasimhan T. N., and Smith A. (1984) "Groundwater contamination from an inactive uranium mill tailings pile: 1. Application of a chemical mixing model." *Water Resources Research* **20**, 1743-1752.

Zachara J. M., Smith S. C., and Kuzel L. S. (1995) "Adsorption and dissociation of Co-EDTA complexes in iron oxide-containing subsurface sands." *Geochimica et Cosmochimica Acta* **59** (No. 23), 4825-4844.